

A comparative analysis of the hominin triquetrum (SKX 3498) from Swartkrans, South Africa

Author:
Tracy L. Kivell¹

Affiliation:
¹Department of Human Evolution, Max Planck Institute of Evolutionary Anthropology, Leipzig, Germany

Correspondence to:
Tracy Kivell

Email:
tracy_kivell@eva.mpg.de

Postal address:
Department of Human Evolution, Max Planck Institute of Evolutionary Anthropology, Deutscher Platz 6, Leipzig 04103, Germany

Dates:
Received: 12 Nov. 2010
Accepted: 08 Feb. 2011
Published: 11 May 2011

How to cite this article:
Kivell TL. A comparative analysis of the hominin triquetrum (SKX 3498) from Swartkrans, South Africa. *S Afr J Sci.* 2011;107(5/6), Art. #515, 10 pages. doi:10.4102/sajs.v107i5/6.515

© 2011. The Authors.
Licensee: OpenJournals Publishing. This work is licensed under the Creative Commons Attribution License.

The SKX 3498 triquetrum from Member 2 at Swartkrans Cave, South Africa is the only hominin triquetrum uncovered (and published) thus far from the early Pleistocene hominin fossil record. Although SKX 3498 was found over two decades ago, its morphology has not been formally described or analysed, apart from the initial description. Furthermore, the taxonomic attribution of this fossil remains ambiguous as both *Paranthropus* and early *Homo* have been identified at Swartkrans. This analysis provides the first quantitative analysis of the SKX 3498 triquetrum, in comparison to those of extant hominids (humans and other great apes) and other fossil hominins. Although the initial description of the SKX 3498 triquetrum summarised the morphology as generally human-like, this analysis reveals that quantitatively it is often similar to the triquetra of all hominine taxa and not necessarily humans in particular. Shared hominid-like morphology between SKX 3498 and Neanderthals suggests that both may retain the symplesiomorphic hominin form, but that functional differences compared to modern humans may be subtle. Without knowledge of triquetrum morphology typical of earlier Pliocene hominins, the taxonomic affiliation of SKX 3498 remains unclear.

Introduction

Between 1979 and 1986 a complete, undistorted hominin right triquetrum (SKX 3498) was discovered from Member 2 at the Pleistocene site of Swartkrans Cave, South Africa (1.8 MYA – 1.0 MYA¹). Susman^{2,3} provided an initial description of this fossil, describing it as ‘essentially humanlike’ in its overall shape and facet morphology and within the size range of ‘small (5’0”) modern humans’. Only the elliptical shape of the pisiform facet was described as being unique and unlike that of modern humans or chimpanzees.^{2,3}

Since this initial description, however, the SKX 3498 triquetrum has been rarely mentioned in the literature, most likely because it is the only early Pleistocene hominin triquetrum known (and published) and little comparative data exist.⁴ Furthermore, because Swartkrans, and Member 2 specifically, are associated with both *Paranthropus robustus* and early *Homo* (*Homo* cf. *erectus*⁵), the taxonomic affiliation of this carpal bone remains uncertain. This analysis provides the first quantitative analysis of this fossil in comparison to the triquetra of modern humans and other great apes (Figure 1) and to published data on hominin fossils (*Ardipithecus ramidus*, *Homo neanderthalensis* and archaic *H. sapiens*), with the aim of clarifying its functional and taxonomic interpretation.

Materials and methods

The qualitative description and measurement of the original SKX 3498 triquetrum were conducted at the Ditsong (formerly Transvaal) National Museum of Natural History in Pretoria, South Africa. SKX 3498 was compared to a large sample ($n = 254$) of extant hominids (humans and other great apes, Table 1). The modern human sample comprised White and Black individuals and was derived from the Grant collection (University of Toronto) and the Terry collection (Smithsonian Institute). The extant great ape comparative sample included *Pan paniscus*, *P. troglodytes*, *Gorilla gorilla*, *G. berengei*, *Pongo pygmaeus* and *P. abelii* and the individual specimens were housed at the following institutions: The Powell-Cotton Museum, Musee Royal de l’ Afrique Centrale, Max-Planck-Institut für evolutionäre Anthropologie, Museum für Naturkunde Berlin, The National Museum of Natural History, Harvard Museum of Comparative Zoology, The Cleveland Museum of Natural History, The Royal Ontario Museum and the University of Toronto.

Comparisons to the few other fossil hominin triquetra were made using published data. Lovejoy et al.⁶ provided two linear measurements for the *Ar. ramidus* triquetrum ARA-VP-6/500-029: the ‘maximum dimension’ and ‘lunate surface breadth’, assumed to be the equivalent of the maximum breadth of the triquetrum body and lunate facet, respectively, in this analysis (Table 2 and Figure 2). Trinkaus⁷ offered several linear measurements for three adult *H. neanderthalensis* triquetra:

TABLE 1a: Details of the sample of extant taxa used in this analysis.

Taxon	Male	Female	Total
<i>H. sapiens</i>	60	61	121
<i>Pan</i>	28	27	55
<i>P. paniscus</i>	10	9	19
<i>P. troglodytes</i>	18	18	36
Gorilla	28	19	47
<i>G. gorilla</i>	24	15	39
<i>G. berengei</i>	4	4	8
Pongo	12	19	31
<i>P. abelii</i>	3	4	7
<i>P. pygmaeus</i>	9	15	24

TABLE 1b: Details of the sample of fossil taxa used in this analysis.

Specimen	Taxon
SKX 3498	<i>P. robustus</i> or <i>H. cf. erectus</i> ? ^{2,3}
ARA-VP-6/500-029	<i>Ar. ramidus</i> ⁶
Shanidar 4	<i>H. neanderthalensis</i> ⁷
Shanidar 5	<i>H. neanderthalensis</i> ⁷
Shanidar 6	<i>H. neanderthalensis</i> ⁷
Dolní Věstonice 3	archaic <i>H. sapiens</i> ⁸
Dolní Věstonice 14	archaic <i>H. sapiens</i> ⁸

complete left triquetra from Shanidar 6 and Shanidar 4, the latter of which has some pathology, and a complete right triquetrum from Shanidar 5 (Table 2a). Finally, Sládek et al.⁸ provided data on two archaic *H. sapiens* specimens, a left triquetrum from the Dolní Věstonice 3 individual and a more complete right triquetrum from Dolní Věstonice 14.

Nine linear measurements were taken to quantify the size of the triquetrum and its articular facets (Figure 2). A geometric mean was used as the size variable and was calculated from the raw measurements for each specimen.⁹ Each linear measurement was divided by the geometric mean of all measurements to create a dimensionless shape ratio.^{10,11} For some fossil hominin specimens, only a few linear measurements were available with which to calculate a geometric mean (e.g. two variables for *Ar. ramidus*). Because a geometric mean is a volume that requires at least three variables,¹² a Spearman rank correlation (r_s) test was used to determine if a geometric mean derived from fewer variables was significantly correlated with the geometric mean derived from the complete set of variables. Spearman rank correlation was used, as opposed to Pearson’s correlation, because it is a more conservative measure when the relationship between two variables is not necessarily linear.¹³ A significant correlation was determined if $r_s > 0.80$ and $p \leq 0.05$.¹³

Differences in shape ratios across extant taxa were assessed using a one-way analysis of variance followed by a Tukey–Kramer post-hoc test for multiple comparisons.¹³ All statistical analyses were run with sexes pooled and results were considered statistically significant at the $p \leq 0.05$ level. Differences in triquetrum shape ratios amongst extant groups

TABLE 2a: Metric data used in this analysis (given in mm) for extant samples.

Data	Gorilla			Homo			Pan			Pongo		
	Mean	s.d.	Range	Mean	s.d.	Range	Mean	s.d.	Range	Mean	s.d.	Range
BTB	18.4	2.4	(14.0–23.3)	15.7	1.4	(12.0–19.6)	13.9	1.1	(10.8–16.4)	18.9	2.7	(14.8–24.5)
HTB	19.3	3.9	(13.4–27.4)	14.7	1.4	(10.6–18.4)	13.3	1.9	(10.4–19.0)	11.4	1.8	(8.7–14.9)
LTB	13.8	1.8	(10.2–17.7)	10.9	1.1	(8.2–13.7)	10.1	1.5	(7.1–14.3)	8.8	1.4	(6.7–11.7)
HTLF	12.7	1.7	(9.7–16.8)	9.5	0.9	(6.5–11.8)	9.6	1.3	(7.5–13.2)	9.1	1.3	(6.4–12.0)
LTLF	11.5	1.5	(8.9–14.8)	9.5	1.1	(6.8–11.9)	8.8	1.2	(5.9–11.7)	8.3	1.3	(5.8–10.8)
BTHF	16.6	2.1	(12.5–21.3)	14.1	1.5	(10.8–17.9)	12.8	1.2	(10.3–15.3)	16.3	2.0	(12.9–20.3)
HTHF	14.4	1.9	(11.3–19.6)	11.2	1.3	(8.2–15.6)	10.4	1.2	(7.3–13.0)	9.7	1.6	(7.3–13.6)
BTPF	13.2	1.9	(7.5–17.9)	9.8	1.2	(5.8–12.6)	11.1	1.6	(7.3–14.7)	9.5	1.4	(7.5–13.3)
LTPF	10.0	1.4	(7.3–13.3)	8.7	1.1	(5.7–11.0)	7.2	0.9	(5.3–9.1)	6.6	1.0	(5.2–9.3)

BTB, maximum mediolateral breadth of triquetrum body; HTB, maximum dorsopalmar height of triquetrum body; LTB, maximum proximodistal length of triquetrum body; HTLF, maximum dorsopalmar height of triquetrum’s lunate facet; LTLF, maximum proximodistal length of triquetrum’s lunate facet; BTHF, maximum mediolateral breadth of triquetrum’s hamate facet; HTHF, maximum dorsopalmar height of triquetrum’s hamate facet; BTPF, maximum mediolateral breadth of triquetrum’s pisiform facet; LTPF, maximum proximodistal length of triquetrum’s pisiform facet; s.d., standard deviation.

TABLE 2b: Metric data used in this analysis (given in mm) for fossil samples.

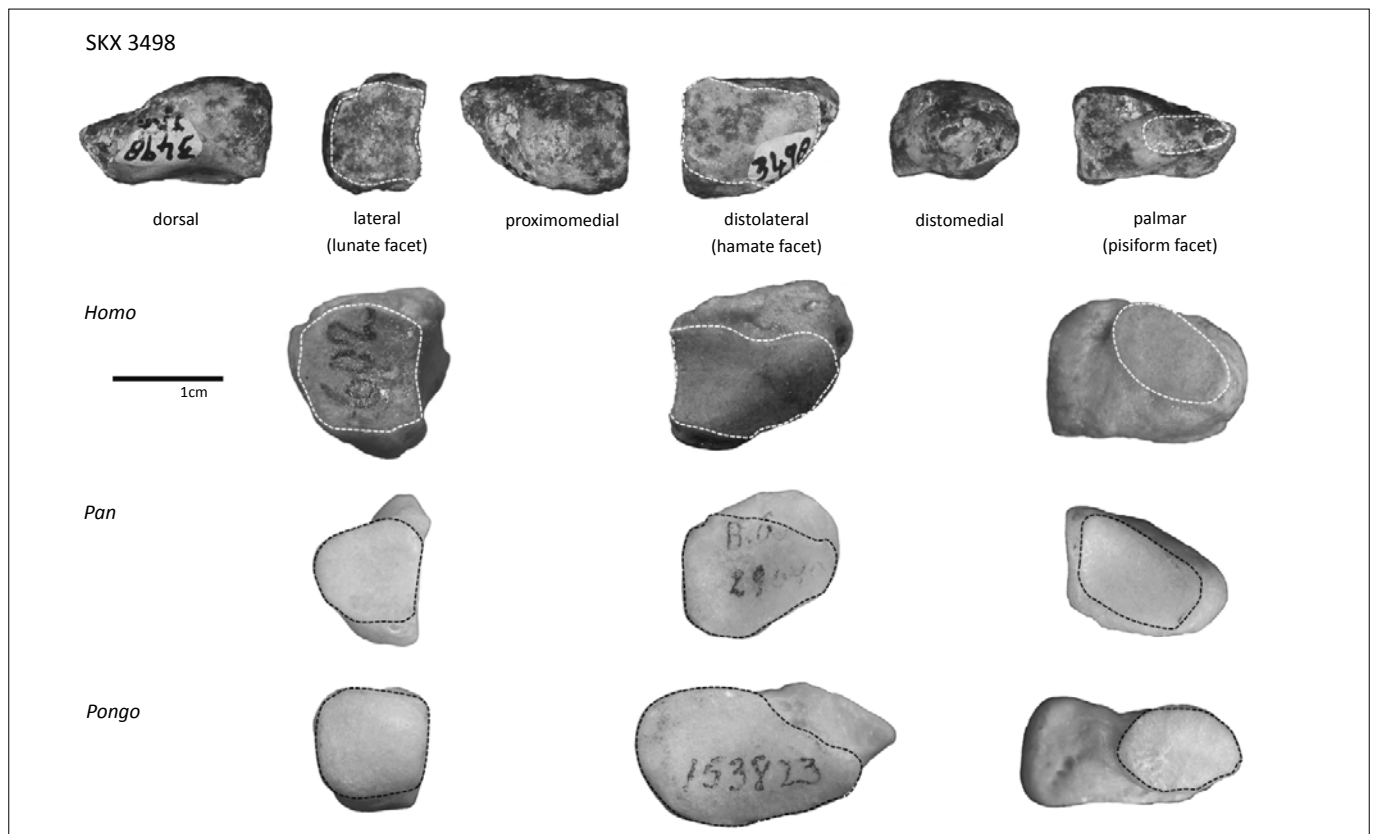
Data	<i>H. neanderthalensis</i> (including Shanidar 4, 5 and 6) ^{7†}			SKX 3498 [‡]	<i>Ar. ramidus</i>	Archaic <i>H. sapiens</i>	
	Mean	s.d.	Range		ARA-VP-6/500-029 ⁶	Dolní Věstonice 3 ⁸	Dolní Věstonice 14 ⁸
BTB	16.0	1.8	(14.0–17.6)	13.0	18.0	13.2	-
HTB	13.4	2.6	(11.2–16.3)	10.8	-	-	14.4
LTB	-	-	-	7.9	-	-	-
HTLF	10.6	1.0	(9.5–11.5)	9.0	-	-	10.0
LTLF	7.4	0.9	(6.4–8.0)	7.5	7.9	-	9.5
BTHF	14	1.6	(12.2–15.2)	11.5	-	-	[15.3]
HTHF	9.1	0.5	(8.8–9.7)	8.8	-	-	11.5
BTPF	8.3	2.7	(6.4–10.2)	7.5	-	8.0	-
LTPF	6.2	1.4	(5.2–7.8)	4.0	-	7.0	9.8

Value in square parentheses is estimated.

BTB, maximum mediolateral breadth of triquetrum body; HTB, maximum dorsopalmar height of triquetrum body; LTB, maximum proximodistal length of triquetrum body; HTLF, maximum dorsopalmar height of triquetrum’s lunate facet; LTLF, maximum proximodistal length of triquetrum’s lunate facet; BTHF, maximum mediolateral breadth of triquetrum’s hamate facet; HTHF, maximum dorsopalmar height of triquetrum’s hamate facet; BTPF, maximum mediolateral breadth of triquetrum’s pisiform facet; LTPF, maximum proximodistal length of triquetrum’s pisiform facet; s.d., standard deviation.

[†], The values presented here include Shanidar 4 for which Trinkaus⁷ notes that there is pathology affecting the measurement for HTB, HTLF, LTLF and HTHF. However, exclusion of Shanidar 4 from these analyses did not substantially alter any of the results and thus all Neanderthal specimens are included here. BTPF is only available for Shanidar 4 and 6 specimens.

[‡], Measurements taken on original fossil.



Articular facets have been outlined in each view.
All triquetra are viewed from the right side and to a 1-cm scale.

FIGURE 1: SKX 3498 triquetrum morphology in comparison to that of extant hominids. SKX 3498 is shown in all views compared to lateral, distolateral and palmar views of *Homo* (male modern *H. sapiens*), *Pan* (female *P. paniscus*) and *Pongo* (male *P. pygmaeus*).

and the fossil sample were evaluated graphically with box-and-whisker plots.

Finally, the morphology of the SKX 3498 triquetrum was further quantitatively compared to the extant sample, Neanderthals and archaic *H. sapiens* Dolní Věstonice 14 using a discriminant function analysis (DFA). DFA is a classification technique that generates a linear combination of variables that maximises the probability of correctly assigning observations into their predetermined groups.¹³ DFA of the extant comparative sample was used to determine the utility of the triquetrum shape ratios to resolve taxonomic and/or functional groups. Subsequently, DFA was also used to assign 'unknown' observations – that is, fossil specimens – into 'a priori-defined' taxonomic groups. Because differences in group sample sizes can bias the discriminant analysis and classification,¹⁴ data were randomly culled to the lowest sample size (i.e. *Pongo*, $n = 31$) to test for any adverse effects.

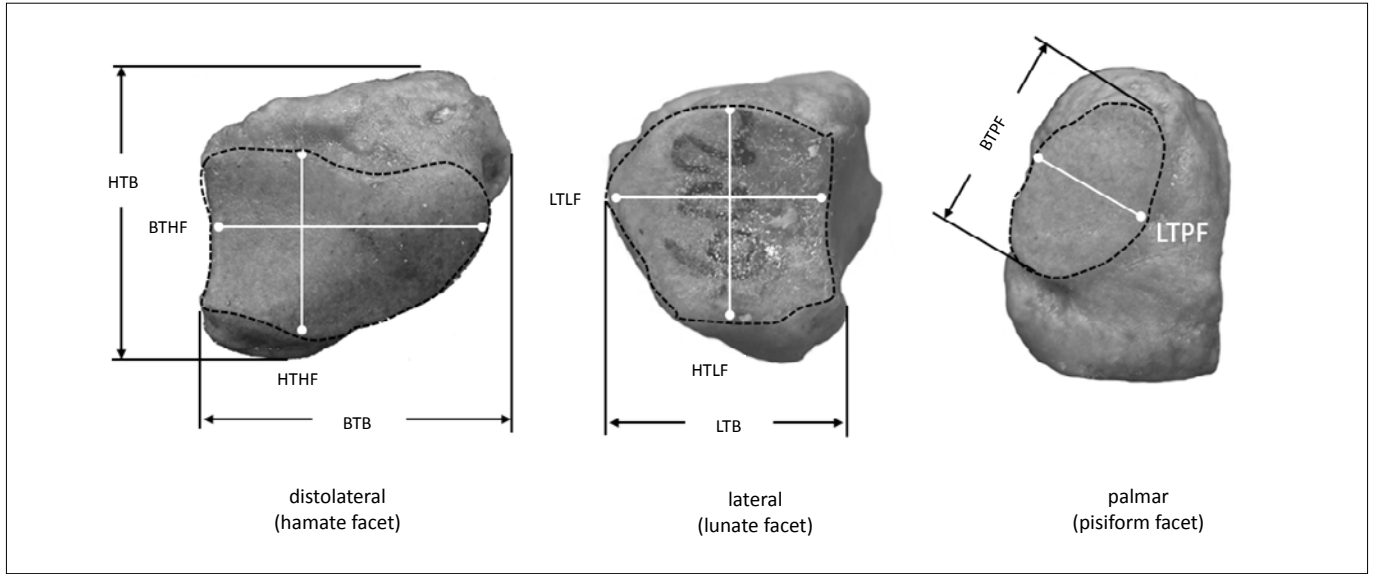
Results

Spearman rank correlation (r_s) revealed that the four additional geometric means calculated from the subsets of variables available for fossil specimens (Table 2b) were significantly correlated with the geometric mean derived from all nine variables: (1) the Neanderthal specimens ($r_s = 0.99$), (2) Dolní Věstonice 14 ($r_s = 0.99$), (3) Dolní Věstonice 3 ($r_s = 0.93$) and (4) *Ar. ramidus* ($r_s = 0.93$). Therefore comparisons across shape ratios are considered robust.

Figure 3 to Figure 6 provide box-and-whisker plots for the relative differences across extant and fossil taxa for each shape ratio. In all cases, the plot including comparisons to the most fossil taxa is shown (i.e. using a shape ratio that is derived from fewer than nine variables) and, unless otherwise stated, the relationships amongst the taxa did not differ substantially from those representing a shape ratio derived from all nine variables. In instances where relationships did change, multiple box-and-whisker plots are shown (e.g. for the maximum breadth of the triquetrum body).

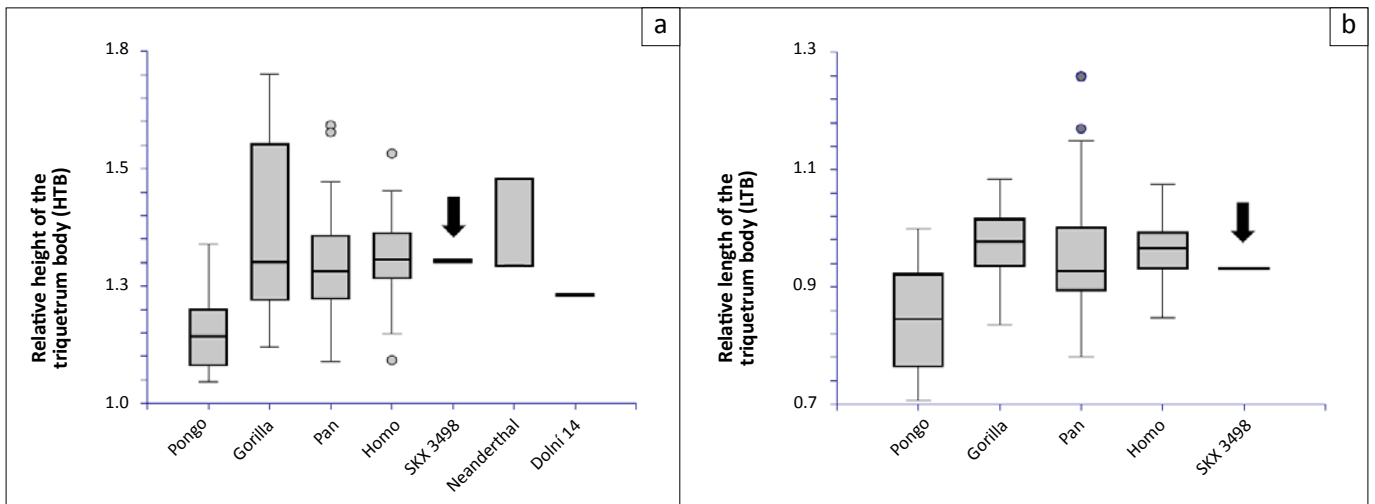
Comparative morphological description of SKX 3498

Previous qualitative descriptions of the SKX 3498 triquetrum described the overall shape of the body and the facet morphology as generally human-like.^{2,3} The results of this analysis generally support this assessment, but morphological similarities are often shared with all hominine taxa (African apes and humans), not just humans, and there are certain aspects of the morphology that are unlike that of humans (Figures 3–6). The SKX 3498 triquetrum body is most similar to hominines in its relative dorsopalmar height, as are Neanderthal and Dolní Věstonice 14 specimens, and in its proximodistal length (Figure 3). However, the mediolateral breadth of the triquetrum body (the longest dimension) is, relative to carpal size, broader than the mean breadth of all extant hominines (Figure 4). The mediolateral breadth of



BTB, maximum mediolateral breadth of triquetrum body; HTB, maximum dorsopalmar height of triquetrum body; LTB, maximum proximodistal length of triquetrum body; HTLF, maximum dorsopalmar height of triquetrum's lunate facet; LTLF, maximum proximodistal length of triquetrum's lunate facet; BTHF, maximum mediolateral breadth of triquetrum's hamate facet; HTHF, maximum dorsopalmar height of triquetrum's hamate facet; BTPF, maximum mediolateral breadth of triquetrum's pisiform facet; LTPF, maximum proximodistal length of triquetrum's pisiform facet.

FIGURE 2: Linear measurements used to quantify the morphology of the SKX 3498 triquetrum.



The black arrow indicates SKX 3498.

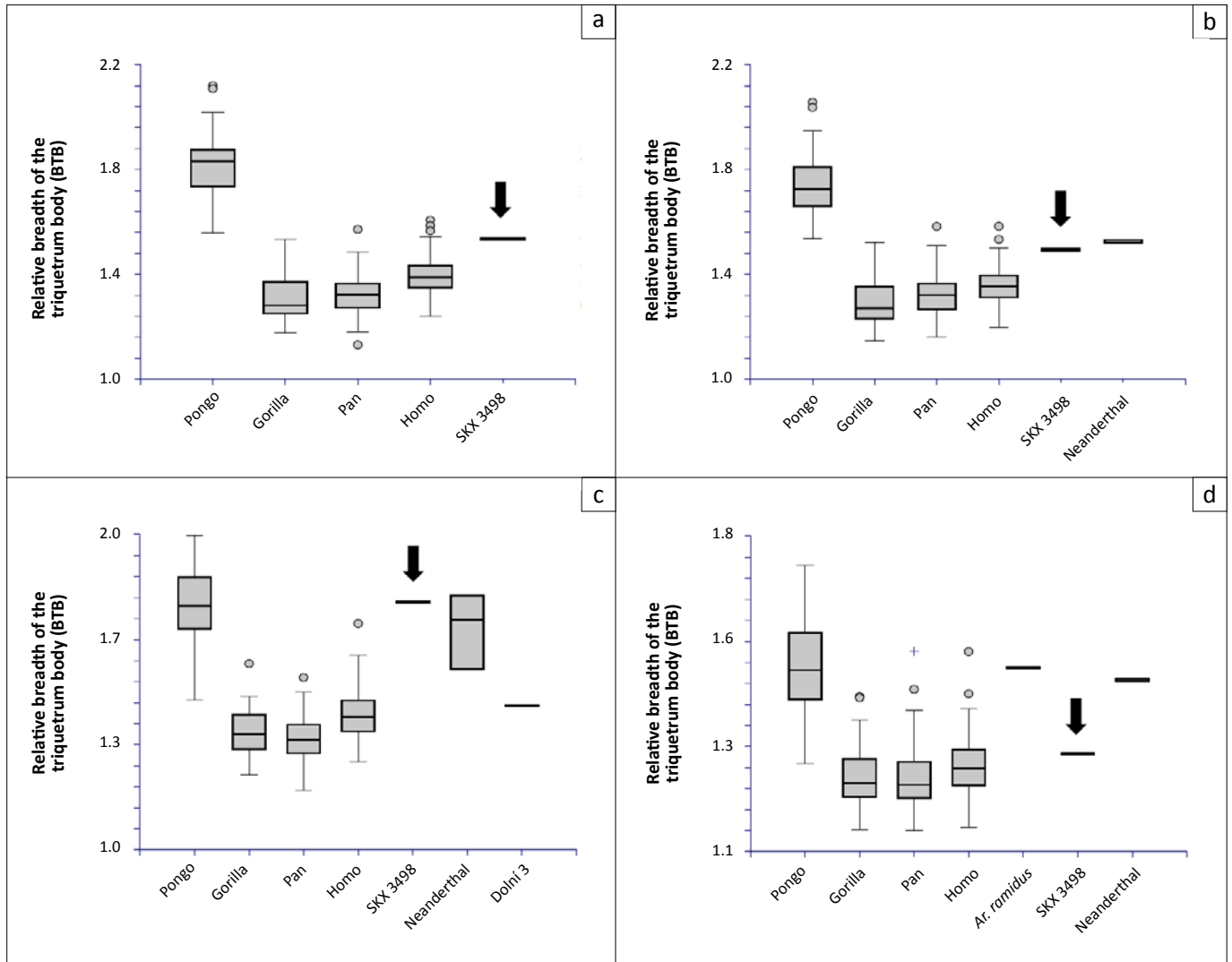
FIGURE 3: Box-and-whisker plots of the relative (i.e. size adjusted) height (a) and length (b) of the triquetrum body in extant and fossil taxa.

SKX 3498 falls outside or within the upper range of variation in breadth in hominines and, in some comparisons, is more similar to *Pongo* (Figure 4c). The broad breadth of SKX 3498 is similar to that of Neanderthals in some quantitative comparisons (Figure 4b and 4c). *Ar. ramidus* also displays a relatively broad triquetrum body (Figure 4d) whilst Dolní Věstonice 3 is most similar to the mean of modern humans (Figure 4c).

The lunate facet of SKX 3498 is similar to extant hominines^{2,3} and other fossil hominins in being slightly concave (unlike *Pongo*, which is strongly convex) and almost square in shape (Figure 1). The relative length of the SKX 3498 lunate facet is similar to that of extant hominines and longer than those of all other fossil hominin taxa (Figure 5a and 5b). However, relative to carpal size, the height of the SKX 3498 lunate facet

is greater than the mean of all extant hominids (humans and other great apes) and Dolní Věstonice 14 and is only within the upper range of variation of *Pan* (Figure 5c). In this way, SKX 3498 is similar to Neanderthals. The SKX 3498 hamate facet is also expansive, with a slight concavo-convex surface that 'wraps around' the dorsomedial edge of the triquetrum body (Figure 2). Relative to carpal size, the breadth of the SKX 3498 hamate facet is greater than the mean of all hominine taxa (but less than that of *Pongo*) and is most similar to that of Neanderthals and, less so, Dolní Věstonice 14 (Figure 5d). The relative height of the hamate facet is also comparatively greater than the mean height of other extant hominid taxa, Neanderthals and Dolní Věstonice 14 (Figure 5e).

The pisiform facet is positioned at the distomedial end of the palmar surface of the triquetrum and its orientation is mostly palmar, but also slightly medially facing (Figure 1). Results of



The black arrow indicates SKX 3498.

FIGURE 4: Box-and-whisker plots of the relative breadth of the triquetrum body (BTB) in extant and fossil taxa. The relative size of the BTB varied depending on the variables used to calculate the geometric mean: the BTB shape ratio derived from all nine variables (a), and from the subset of variables available for Neanderthal specimens (b), Dolní Věstonice 3 (c) and *Ar. ramidus* (d).

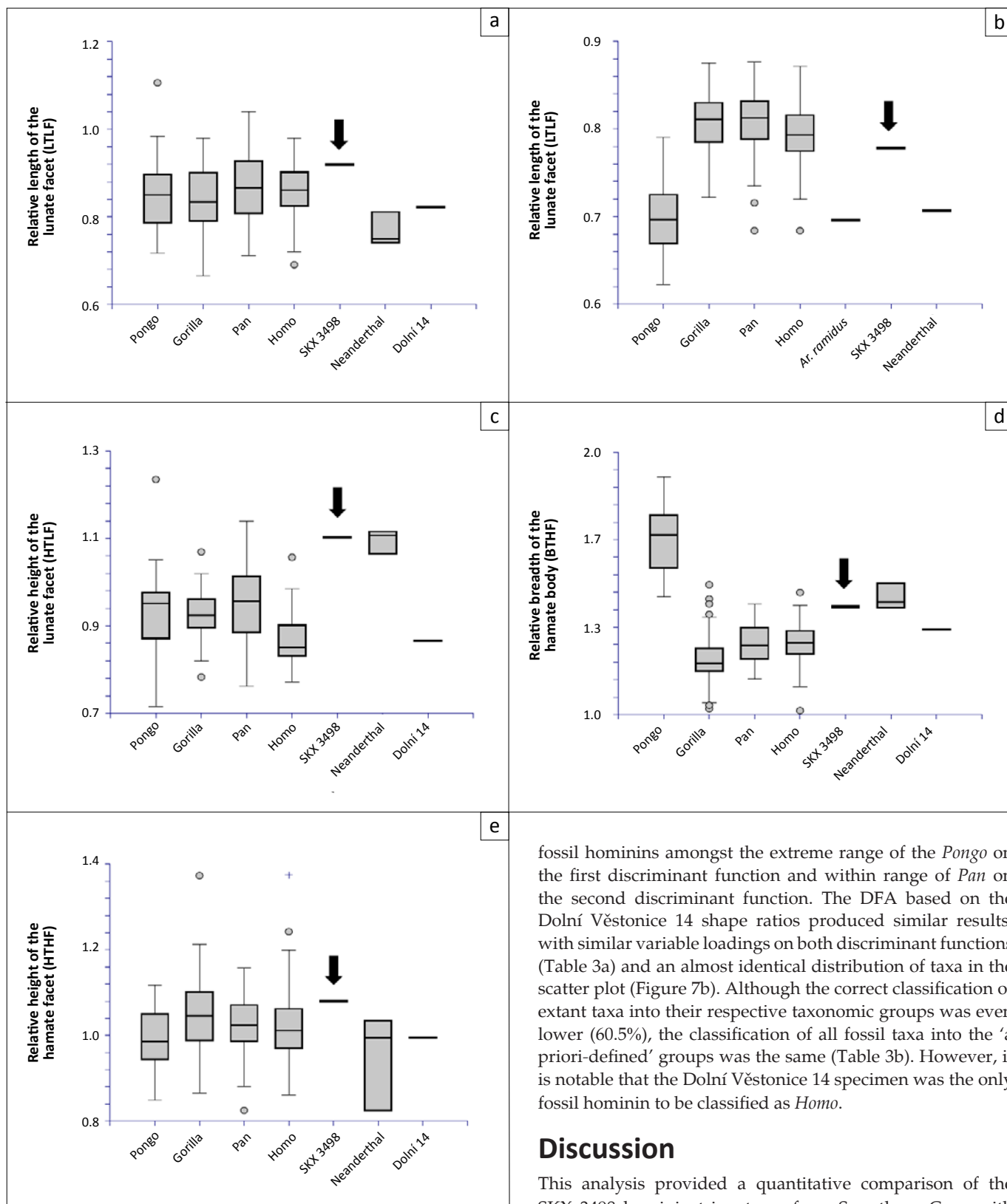
this analysis support Susman's^{2,3} description of the SKX 3498 pisiform facet as being relatively small compared to other hominids. The longest axis (which is almost mediolateral) of the pisiform facet is most similar to African apes in being relatively long and falls outside the range of variation seen in modern humans and other fossil hominins (Figure 6a). However, proximodistally the pisiform facet is uniquely short, falling outside the range of all extant taxa, Neanderthals and Dolní Věstonice 14 (Figure 6b). This combination in SKX 3498 produces an elliptically shaped facet that is unlike the more circular facet of extant hominins.^{2,3} The palmar surface is also marked by a deep groove at the distolateral end for the attachment of a well-developed lunatotriquetrum ligament, which appears similar to that of *Ar. ramidus*⁶ and some modern human specimens, but is unlike the morphology of non-human great apes (Figure 1).

Results of discriminant function analyses

Two DFA were conducted, each based on the subset of shape ratios available for the Neanderthal and Dolní Věstonice 14

specimens (Table 2b). The DFA results on the culled data set yielded the same shape ratio loadings on each discriminant function, a similar distribution of taxa in the scatter plot and the same taxonomic classification of the fossils as the DFA using the complete sample. Therefore, because a larger sample provides a better representation of the natural variation within a given taxon, only the results based on DFA of the complete sample are discussed here.

In the DFA based on the Neanderthal shape ratios, the first discriminant function distinguished *Pongo* from all other hominines because of its relatively broad triquetrum body and hamate facet and relatively short triquetrum body and long pisiform facet (Table 3a, Figure 7a). The second discriminant function distinguished most *Pan* and *Gorilla* specimens from *Homo* specimens by their relatively tall lunate facet and short pisiform facet. Extant taxa were correctly classified into their respective taxonomic groups at only 64.3%. SKX 3498 and all Neanderthal specimens were strongly classified as either *Pongo* or *Pan* (Table 3b), which reflects the placement of all



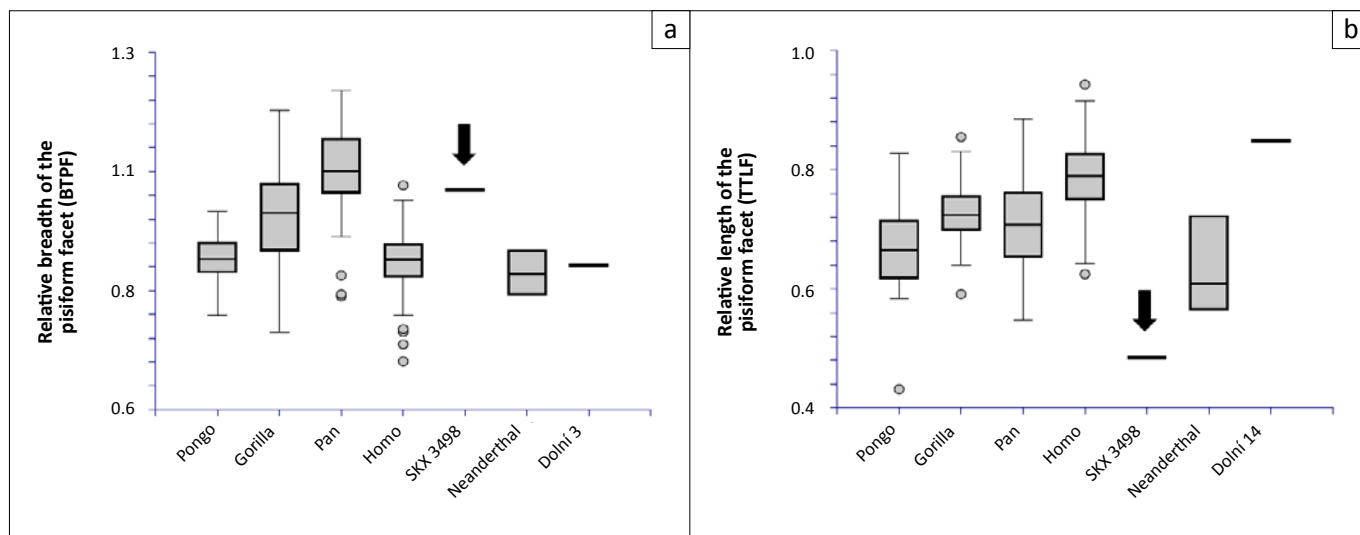
The black arrow indicates SKX 3498.

FIGURE 5: Box-and-whisker plots of the relative size of the triquetrum’s lunate and hamate facets in extant and fossil taxa. The relative length of the lunate facet was derived from the subset of variables available for the Dolní Věstonice 14 (a) and *Ar. ramidus* (b) specimens. The relative height of the lunate facet (c) and the relative breadth (d) and height (e) of the hamate facet were derived from the subset of variables available for the Dolní Věstonice 14 specimen.

fossil hominins amongst the extreme range of the *Pongo* on the first discriminant function and within range of *Pan* on the second discriminant function. The DFA based on the Dolní Věstonice 14 shape ratios produced similar results, with similar variable loadings on both discriminant functions (Table 3a) and an almost identical distribution of taxa in the scatter plot (Figure 7b). Although the correct classification of extant taxa into their respective taxonomic groups was even lower (60.5%), the classification of all fossil taxa into the ‘a priori-defined’ groups was the same (Table 3b). However, it is notable that the Dolní Věstonice 14 specimen was the only fossil hominin to be classified as *Homo*.

Discussion

This analysis provided a quantitative comparison of the SKX 3498 hominin triquetrum from Swartkans Cave with the triquetra of extant hominids and other fossil hominins. Susman’s^{2,3} original description of this fossil summarised the morphology as generally human-like. The quantitative analyses presented here reveal that the morphology of SKX 3498 often is similar to that of extant hominines, but not



The black arrow indicates SKX 3498.

FIGURE 6: Box-and-whisker plots of the relative size of the triquetrum's pisiform facet in extant and fossil taxa. The relative breadth of the pisiform facet was derived from the subset of variables available for the Dolní Věstonice 3 specimen (a) and the relative length was derived from variables available for the Dolní Věstonice 14 specimen (b).

specifically humans. Relative to carpal size, the height and length of the SKX 3498 triquetrum body, the shape of the lunate facet, and some aspects of the hamate and pisiform facets are similar to both modern humans and African apes. The relative breadth of the SKX 3498 triquetrum body and its hamate facet are intermediate between that of hominines and *Pongo*, whilst the length of the pisiform facet is uniquely short, as described by Susman^{2,3}, compared to all other extant and fossil taxa. Neanderthals share much of this morphology with SKX 3498, but have a more *Pongo*-like hamate facet and length of the lunate facet relative to carpal size. The two morphometric variables available for *Ar. ramidus* are more similar to *Pongo* whilst Dolní Věstonice 3 and 14 are more similar to modern humans.

Both SKX 3498 and all Neanderthal specimens were strongly classified in the DFA as non-human hominids, despite having morphology that has been generally described qualitatively as human-like.^{2,3,7} In addition, the three Neanderthal triquetra are classified as different taxa (*Pan* vs. *Pongo*), despite being from the same taxon and the same site (Shanidar Cave).⁷ Although this result is consistent with the many similarities in relative size of the triquetrum body and facet morphology of these fossil specimens to those of hominines or *Pongo*, the results are likely confounded by three methodological factors. Firstly, many of the shape ratios that distinguished *Pongo* from extant hominine taxa – namely the broader triquetrum body and hamate facet and shorter pisiform facet – are also shape ratios in which both SKX 3498 and the Neanderthal specimens are quantitatively (i.e. relative to carpal size) more similar to *Pongo*. Secondly, in DFA the unique or intermediate morphology of SKX 3498 and Neanderthals *must* be classified into 'a priori-defined' group. Thirdly, the triquetrum measurements used in this study were poor in distinguishing amongst extant taxonomic or functional groups and, in particular, the more subtle variation amongst hominine triquetrum morphology. Thus, although qualitative comparisons describe the morphology

TABLE 3a: Results from two discriminant function analyses (DFA) based on shape ratios available for Neanderthal and Dolní Věstonice 14 specimens: Correlations of prediction variables with discriminant functions.

Results	Neanderthal DFA		Dolní Věstonice 14 DFA	
	Function 1	Function 2	Function 1	Function 2
Ratios				
Eigenvalue	5.02	0.55	3.46	0.41
Individual %	88.6	9.60	87.80	10.30
Canonical correlation	0.91	0.59	0.88	0.54
Variable				
BTB	0.71 [†]	0.45	-	-
HTB	-0.28 [†]	-0.21	-0.28 [†]	-0.19
HTLF	-0.02	-0.83 [†]	0.12	-0.86 [†]
LTLF	-0.09	-0.02	-0.01	0.05
BTHF	0.62 [†]	0.24	0.86 [†]	0.36
HTHF	-0.16	-0.25	-0.09	-0.23
LTPF	-0.26 [†]	0.61 [†]	-0.25 [†]	0.73 [†]

[†], The highest and lowest loading variables on each function. BTB, maximum mediolateral breadth of triquetrum body; HTB, maximum dorsopalmar height of triquetrum body; HTLF, maximum dorsopalmar height of triquetrum's lunate facet; LTLF, maximum proximodistal length of triquetrum's lunate facet; BTHF, maximum mediolateral breadth of triquetrum's hamate facet; HTHF, maximum dorsopalmar height of triquetrum's hamate facet; LTPF, maximum proximodistal length of triquetrum's pisiform facet.

TABLE 3b: Results from two discriminant function analyses (DFA) based on shape ratios available for Neanderthal and Dolní Věstonice 14 specimens: Predicted classification of fossil specimens.

Specimen	Taxon	Predicted taxonomic group (%)
Neanderthal DFA		
SKX 3498	?	<i>Pongo</i> (99.6%)
Shanidar 4	<i>H. neanderthalensis</i>	<i>Pan</i> (75.1%), <i>Gorilla</i> (19.4%)
Shanidar 5	<i>H. neanderthalensis</i>	<i>Pongo</i> (99.3%)
Shanidar 6	<i>H. neanderthalensis</i>	<i>Pan</i> (88.8%), <i>Pongo</i> (6.7%)
Dolní Věstonice 14 DFA		
SKX 3498	?	<i>Pongo</i> (97.5%)
Shanidar 4	<i>H. neanderthalensis</i>	<i>Pan</i> (67.2%), <i>Gorilla</i> (25.0%)
Shanidar 5	<i>H. neanderthalensis</i>	<i>Pongo</i> (97.7%)
Shanidar 6	<i>H. neanderthalensis</i>	<i>Pan</i> (80.1%), <i>Pongo</i> (13.7%)
Dolní Věstonice 14	archaic <i>H. sapiens</i>	<i>Homo</i> (76.3%), <i>Pan</i> (13.9%)

of SKX 3498^{2,3} (Figure 1) and Neanderthals⁷ as generally human-like, this similarity was not captured by the linear measurements used in this analysis. It is possible that with the inclusion of angles of orientation, curvature or surface

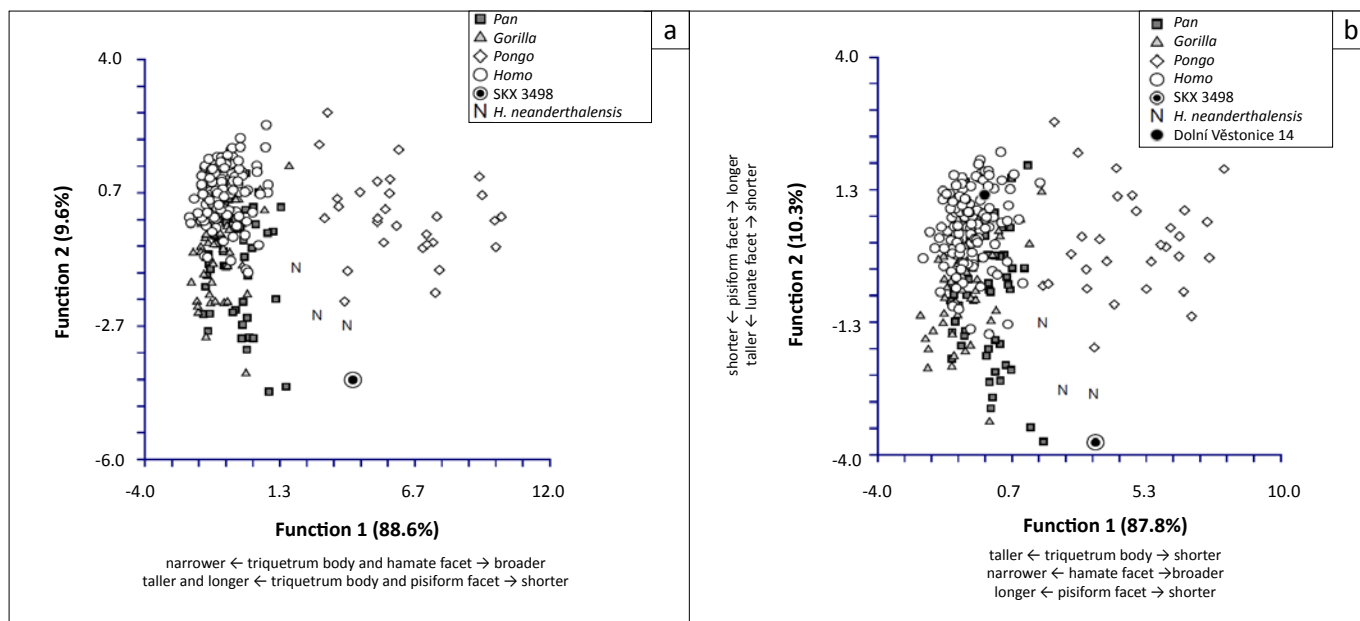


FIGURE 7: Scatter plots of the first two discriminant functions based on the shape ratios available for (a) the Neanderthal specimens and (b) the Dolní Věstonice 14 specimen.

area of facets, for example, the variation amongst extant hominines and the more human-like aspects of fossil hominin triquetrum morphology may be revealed.

Despite these methodological limitations, it is notable that the Dolní Věstonice 14 specimen was correctly classified as *H. sapiens* in the DFA, suggesting that: (1) the measurements used in this analysis were robust enough to distinguish human from non-human triquetrum morphology and (2) the non-human classification of SKX 3498 and the Neanderthal specimens reflects, at least to some degree, true morphological differences from those of archaic or modern humans that have not been previously recognised. Thus, the evolutionary implications of these results need to be further explored.

Functional implications

The SKX 3498 triquetrum, as well as those of Neanderthals and *Ar. ramidus*, is relatively more mediolaterally broad than modern humans and African apes. A relatively broad triquetrum body suggests that the functional role of the pisiform could have been more accentuated compared to that of humans. The pisiform serves as an attachment site for the tendon of the flexor carpi ulnaris muscle and the shape, size and position of the pisiform can alter the moment arm of this muscle.^{15,16} Relative to humans, the broader body of SKX 3498 would move the already distomedially placed pisiform facet more distomedially, which, depending on the morphology of the pisiform, could increase the flexion and adduction moment arm of the flexor carpi ulnaris muscle. However, such a functional hypothesis depends strongly on the size and shape of the pisiform.

SKX 3498 has a unique elliptically shaped pisiform facet^{2,3} – morphology that is not found in any of the extant or fossil taxa in this sample. Unfortunately, little is known about the relationship between the pisiform facet of the triquetrum

and the shape of the pisiform itself and there is a paucity of both bones in the hominin fossil record. Thus the functional implications that can be derived from the shape of the triquetrum’s pisiform articulation are limited. The unique pisiform facet in SKX 3498 suggests that the shape of the pisiform may have been different from the more circular, small, pea-shaped pisiform of archaic⁸ and modern humans and Neanderthals.⁷ However, it cannot be presumed that the pisiform associated with the SKX 3498 triquetrum was elongated and rod-shaped like that of *Au. afarensis*^{17,18} and great apes. The corresponding triquetrum facet of the *Au. afarensis* pisiform appears more circular than the equivalent pisiform facet on the SKX 3498 triquetrum,¹⁷ suggesting that the associated pisiform of SKX 3498 was different from that of *Au. afarensis*. Variation in pisotriquetrum facet shapes may instead reflect the degree of movement at this joint, rather than the shape of the pisiform itself. The synovial pisotriquetrum joint permits a large degree of movement in the pisiform, being pulled by the attached ligaments and tendons proximally during flexion and adduction and distally during extension and abduction.¹⁵ Thus the functional implications, if any, of the unique SKX 3498 pisiform facet morphology remain unclear.

The relatively expansive lunate and hamate facets suggest that the SKX 3498 morphology may have allowed for slightly more mobility at the lunatotriquetrum and hamatotriquetrum joints than is typically found in extant hominines. Although the triquetrum is firmly bound within the carpus via extrinsic and intrinsic ligaments to the distal ulna and adjacent carpals, it is still capable of a large degree of movement within the wrist.^{19,20} The relatively broad hamate facet suggests that the triquetrum may have been able to move into a more extreme mediolateral position, rotating along the convex surface of the hamate, allowing for greater ulnar deviation than is typically found in hominines.²⁰ For example, *Pongo*, with the broadest hamate facet in the sample, has a much larger range of ulnar deviation (98 degrees²¹) than the narrower facets of *Pan* (70 degrees²¹) or *Homo* (38 degrees²²). However, without



knowledge of the mutual facets on the lunate and hamate or soft tissue morphology, inferring mobility in these joints remains speculative. Given that the breadth of the hamate facet of the SKX 3498 triquetrum and that of Neanderthals fall within the upper range of the variation in breadth in hominines, the degree of ulnar deviation in fossil hominins was likely more similar to that of modern humans or African apes than to the extreme mobility of *Pongo*.

It is similarly challenging to interpret the functional significance of the SKX 3498 morphology in terms of tool-use or tool-making capabilities as the triquetrum is rarely discussed in the analyses of hominin hand use. This absence in the literature is likely as a result of the scarcity of triquetra in the early hominin fossil record, though new discoveries of relatively complete australopithecine hands at Sterkfontein (2.2 MYA^{23,24,25}) and Malapa (1.8 MYA^{26,27}) in South Africa promise to offer a more comprehensive perspective on overall hominin hand function. Much of the research on hominin wrist and hand function has, understandably, focused on the interface between the distal carpal row and the metacarpals.^{6,18,28,29,30,31,32,33,34,35} Analyses of the nearly complete wrists of *Ar. ramidus*⁶ or Neanderthal and early *H. sapiens*^{28,33,34} do not specifically discuss the functional morphology of the triquetrum. Thus, direct comparisons to other hominin triquetra are challenging. However, given (1) the general quantitative similarities between SKX 3498 and Neanderthal triquetra in this analysis and (2) that Neanderthal hand morphology overall has been interpreted as generally like that of modern humans and indicative of modern human manipulative capabilities,^{7,28,33,34} it is reasonable to assume that the morphological variation in triquetrum morphology between SKX 3498/Neanderthals and humans implies relatively subtle functional differences within the wrist as a whole. That said, recent experimental analyses have shown that the wrist plays a particularly important role in the biomechanics of stone tool production³⁶ and that the intrinsic muscles of the fifth digit, not just the muscles of the thumb and index finger, are important for tool use³⁷ (but see Williams and Richmond³⁸). Thus, further functional studies of the medial wrist bones, particularly the triquetrum and pisiform, may offer new insight into the hand use of early hominins.

The limited data available for *Ar. ramidus* (4.4 MYA),⁶ as well as much of the morphology of SKX 3498 (1.8 MYA – 1.0 MYA¹) and the Shanidar Neanderthal specimens (approximately 0.11 MYA – 0.04 MYA^{7,39}), are similar to non-human hominids and are distinct from the Dolní Věstonice specimens (0.03 MYA⁸) and modern humans. This division suggests that the triquetrum morphology documented in *Ar. ramidus*, SKX 3498 and Neanderthals may be symplesiomorphic for fossil hominins and that the more derived form of archaic and modern humans may be a relatively recent development in human evolutionary history.

Taxonomic implications

Unfortunately this analysis provides little resolution regarding the taxonomic attribution of the SKX 3498 triquetrum. Both *P. robustus* and early *Homo* (*Homo cf.*

*erectus*⁵) have been identified at Swartkrans and in Member 2 specifically^{1,5} and these results demonstrate that SKX 3498 could be attributed to either of these taxa (or to an as yet unidentified hominin taxon). The similarities to Neanderthal morphology might suggest that SKX 3498 is more likely to be early *Homo* rather than *P. robustus*. However, it is unclear if both SKX 3498 and Neanderthals simply retain symplesiomorphic hominin morphology common to many hominin taxa or if earlier hominins (e.g. australopithecines and paranthropines) had a different, more great-ape-like morphology from which SKX 3498 and Neanderthals have derived. Given the modern human-like morphology of the Dolní Věstonice specimens relative to the other fossil hominins in this analysis, it may be more likely that similarities between SKX 3498 and Neanderthals are primitive hominin retentions and that modern human-like triquetrum morphology has evolved relatively recently (i.e. within *H. sapiens* only). In such a scenario, the SKX 3498 could be either *P. robustus* or early *Homo*. Unfortunately the available information on the *Ar. ramidus* triquetrum is not sufficient to establish the morphotype of a potential last common ancestor of *Homo-Pan*.^{6,40} Until descriptions of australopithecine triquetra from Sterkfontein^{23,24} and Malapa²⁶ are available, the evolution of hominin triquetrum morphology and the taxonomic affiliation of SKX 3498 remain ambiguous.

Conclusion

The initial description of the SKX 3498 triquetrum summarised its morphology as human-like, with a unique pisiform facet.^{2,3} This analysis generally supports this description, but reveals that the SKX 3498 morphology is most similar to all extant hominine taxa and not specifically humans. In this way, SKX 3498 shares much of its morphology with Neanderthals and both are often distinct from archaic *H. sapiens* Dolní Věstonice specimens and modern humans. Despite the methodological limitations of this study, the quantitative distinction made between archaic and modern *H. sapiens*, on the one hand, and SKX 3498 and Neanderthals (and the limited data available for *Ar. ramidus*) on the other hand, suggests true morphological differences between the latter specimens and *H. sapiens* that have not been previously recognised.^{2,3,7} The triquetrum morphology of SKX 3498 and Neanderthals may be considered symplesiomorphic for fossil hominins whilst the morphology found in *H. sapiens* likely evolved relatively recently in hominin evolution. Functional interpretations of the SKX 3498 morphology are tentative, but may suggest slightly more mobility at the triquetrolunate and triquetrohamate joints and an enhanced function of the pisiform and flexor carpi ulnaris muscle than is found in modern humans. However, the morphological similarities between SKX 3498 and Neanderthals, for which in the latter numerous wrist bones are known and overall wrist function is considered generally human-like,^{7,28,33,34} imply relatively subtle functional differences between fossil hominin and modern human triquetra. Without a clearer understanding of triquetrum morphology in earlier hominins, the taxonomic affiliation of the SKX 3498 triquetrum remains unknown.



Acknowledgements

I am grateful for the support and hospitality of Stephany Potze and Dr. Martin Kruger of the Ditsong (Transvaal) National Museum of Natural History and for making SKX 3498 available for study. I am also grateful to the following curators from whom the comparative sample was obtained: W. Wendelen and M. Louette (Musée royal de l'Afrique centrale), F. Mayer and S. Jancke (Museum für Naturkunde Berlin), U. Schwartz (Max-Planck-Institut für evolutionäre Anthropologie), M. Harman (Powell-Cotton Museum), L. Gordon (Smithsonian Institution), Y. Haile-Selassie and L. Jellema (Cleveland Museum of Natural History), and J. Eger and S. Woodward (Royal Ontario Museum). Finally, I am thankful to two anonymous reviewers for constructive comments, Matthew Skinner for helpful discussions that improved this manuscript and Jean-Jacques Hublin for research support. This research was funded by the Natural Sciences Engineering Research Council of Canada, General Motors Women in Science and Mathematics and the Max Planck Society.

References

- Brain CK. Structure and stratigraphy of the Swartkrans cave in light of the new excavations. In: Brain CK, editor. *Swartkrans: A cave's chronicle of early man*. Pretoria: Transvaal Museum, 1993; p. 23–34.
- Susman RL. New postcranial remains from Swartkrans and their bearing on the functional morphology and behaviour of *Paranthropus robustus*. In: Grine FE, editor. *Evolutionary history of the 'robust' australopithecines*. New York: Aldine de Gruyter, 1988; p. 149–172.
- Susman RL. New hominid fossils from the Swartkrans formation (1979–1986 excavations): Postcranial specimens. *Am J Phys Anthropol*. 1989;79:451–474. doi:10.1002/ajpa.1330790403, PMID:2672829
- Tocheri MW, Orr CM, Jacofsky MC, Marzke MW. The evolutionary history of the hominin hand since the last common ancestor of *Pan* and *Homo*. *J Anat*. 2008;212:544–562. doi:10.1111/j.1469-7580.2008.00865.x, PMID:18380869, PMCID:2409097
- Susman RL, de Ruiter D, Brain CK. Recently identified postcranial remains of *Paranthropus* and early *Homo* from Swartkrans Cave, South Africa. *J Hum Evol*. 2001;41:607–629. doi:10.1006/jhev.2001.0510, PMID:11782111
- Lovejoy CO, Simpson SW, White TD, Asfaw B, Suwa G. Careful climbing in the Miocene: The forelimbs of *Ardipithecus ramidus* and humans are primitive. *Science*. 2009;326:70e1–70e8.
- Trinkaus E. *The Shanidar Neandertals*. New York: Academic Press; 1983.
- Sládek V, Trinkaus E, Hillson SW, Holliday TW. The people of the Pavlovian: Skeletal catalogue and osteometrics of the Gravettian fossil hominids from Dolní Věstonice and Pavlov. *Dolní Věstonice Studies* 5. Brno: Akademie věd České republiky; 2000.
- Jungers WL, Falsetti AB, Wall CE. Shape, relative size and size-adjustments in morphometrics. *Yrbk Phys Anthropol*. 1995;38:137–161. doi:10.1002/ajpa.1330380608
- Mossiman JE. Size allometry: Size and shape variables with characterizations of the lognormal and generalized gamma distributions. *J Am Stat Assoc*. 1970;56:930–945.
- Darroch JN, Mosimann JE. Canonical and principal components of shape. *Biometrika*. 1985;72:241–252. doi:10.1093/biomet/72.2.241
- Coleman MN. What does geometric mean, mean geometrically? Assessing the utility of geometric mean and other size variables in studies of skull allometry. *Am J Phys Anthropol*. 2007;135:404–415. doi:10.1002/ajpa.20761, PMID:18067122
- Quinn GP, Keough MJ. *Experimental design and data analysis for biologists*. Cambridge: Cambridge University Press; 2002.
- Sanchez PM. The unequal group size problem in discriminant analysis. *J Acad Marketing Sci*. 1974;102:629–633. doi:10.1007/BF02729456
- Taleisnik J. *The wrist*. New York: Churchill Livingstone; 1985.
- Hamrick MW. Functional osteology of the primate carpus with special reference to Strepsirhini. *Am J Phys Anthropol*. 1997;104:105–116. doi:10.1002/(SICI)1096-8644(199709)104:1<105::AID-AJPA7>3.0.CO;2-Q
- Bush ME, Lovejoy CO, Johanson DC, Coppens Y. Hominid carpal, metacarpal and phalangeal bones recovered from the Hadar Formation: 1974–1977 collections. *Am J Phys Anthropol*. 1982;57:651–677. doi:10.1002/ajpa.1330570410
- Marzke MW. Joint functions and grips of the *Australopithecus afarensis* hand, with special reference to the region of the capitate. *J Hum Evol*. 1983;12:197–211. doi:10.1016/S0047-2484(83)80025-6
- Feipel V, Rooze M, Louryan S, Lemort M. Functional anatomy of the carpus in flexion and extension and in radial and ulnar deviations: An *in vivo* two- and three-dimensional CT study. In: Schuind F, An K-N, Cooney WP III, Garcia-Elias M, editors. *Advances in the biomechanics of the hand and wrist*. New York: Plenum Press, 1994; p. 255–270.
- Moritomo H, Goto A, Yoshinobu S, Sugamoto K, Murase T, Yoshikawa H. The triquetrum-hamate joint: An anatomic and *in vivo* three-dimensional kinematic study. *J Hand Surg*. 2003;28A(5):797–805.
- Tuttle RH. Terrestrial trends in the hands of the Anthropoidea. *Proceedings of the 2nd International Congress of Primatology*; 1968; Atlanta, GA, USA. Basel: S. Karger; 1969. p. 192–200.
- Ryu J, Palmer AK, Cooney WP III. Wrist joint motion. In: An K-N, Berger RA, Cooney WP III, editors. *Biomechanics of the wrist joint*. New York: Springer-Verlag, 1991; p. 37–60.
- Clarke RJ. Discovery of complete arm and hand of the 3.3 million-year-old *Australopithecus* skeleton from Sterkfontein. *S Afr J Sci*. 1999;95:477–480.
- Clarke RJ. Latest information on Sterkfontein's *Australopithecus* skeleton and a new look at *Australopithecus*. *S Afr J Sci*. 2008;104:443–449. doi:10.1590/S0038-23532008000600015
- Pickering R, Kramers JD. Re-appraisal of the stratigraphy and determination of new U-Pb dates for the Sterkfontein hominin site, South Africa. *J Hum Evol*. 2010;59:70–86. doi:10.1016/j.jhev.2010.03.014, PMID:20605190
- Berger LR, DeRuiter DJ, Churchill SE, et al. *Australopithecus sediba*: A new species of *Homo*-like australopithecine from South Africa. *Science*. 2010;328:195–204. doi:10.1126/science.1184944, PMID:20378811
- Dirks PHGM, Kibii JM, Kuhn BF, et al. Geological setting and age of *Australopithecus sediba* from Southern Africa. *Science*. 2010;328:205–208. doi:10.1126/science.1184950, PMID:20378812
- Niewoehner WA, Weaver AH, Trinkaus E. Neandertal capitate-metacarpal articular morphology. *Am J Phys Anthropol*. 1997;103:219–233. doi:10.1002/(SICI)1096-8644(199706)103:2<219::AID-AJPA7>3.0.CO;2-O
- Ricklan DE. Functional anatomy of the hand of *Australopithecus africanus*. *J Hum Evol*. 1987;16:643–664. doi:10.1016/0047-2484(87)90018-2
- Marzke MW. Precision grips, hand morphology and tools. *Am J Phys Anthropol*. 1997;102:91–110. doi:10.1002/(SICI)1096-8644(199701)102:1<91::AID-AJPA8>3.0.CO;2-G
- Marzke MW, Wullsetin KL, Viegas SF. Evolution of the power (squeeze grip) and its morphological correlates in hominids. *Am J Phys Anthropol*. 1992;89:283–298. doi:10.1002/ajpa.1330890303, PMID:1485637
- Marzke MW, Marzke RF. Evolution of the human hand: Approaches to acquiring, analysing and interpreting the anatomical evidence. *J Anat*. 2000;197:121–140. doi:10.1046/j.1469-7580.2000.19710121.x, PMID:10999274, PMCID:1468111
- Niewoehner WA. The functional anatomy of late Pleistocene and recent human carpometacarpal and metacarpophalangeal articulations. PhD thesis, Albuquerque, University of New Mexico, 2000.
- Niewoehner WA. Behavioral inferences from the Skhul/Qafzeh early modern human hand remains. *Proc Natl Acad Sci*. 2001;98(6):2979–2984. doi:10.1073/pnas.041588898, PMID:11248017, PMCID:30592
- Tocheri MW, Marzke MW, Liu D, et al. Functional capabilities of modern an fossil hominid hands: Three-dimensional analysis of trapezia. *Am J Phys Anthropol*. 2003;122:101–112. doi:10.1002/ajpa.10235, PMID:12949830
- Williams EM, Gordon AD, Richmond BG. Upper limb kinematics and the role of the wrist during stone tool production. *Am J Phys Anthropol*. 2010;143:134–145. doi:10.1002/ajpa.21302, PMID:20734439
- Marzke MW, Toth N, Schick K, et al. EMG study of hand muscle recruitment during hard hammer percussion manufacture of Oldowan tools. *Am J Phys Anthropol*. 1998;105:315–332. doi:10.1002/(SICI)1096-8644(199803)105:3<315::AID-AJPA3>3.0.CO;2-Q
- Williams EM, Richmond BG. Hand pressure during Oldowan stone tool production. *Am J Phys Anthropol*. 2010;141:243.
- Solecki RS. Shanidar IV, a Neanderthal flower burial in northern Iraq. *Science*. 1975;190:880–881.
- Sarmiento EE. Comment on the palaeobiology and classification of *Ardipithecus ramidus*. *Science*. 2010;328:1105b. doi:10.1126/science.1184148, PMID:20508113